Electronic Supplementary Material (ESI) for Materials Horizons.

Supplementary Information

Ultra High performance, lead free Bi_2WO_6: P(VDF-TrFE) based triboelectric nanogenerator for self-powered sensor and smart electronic applications

Dhiraj Kumar Bharti[1], Sushmitha Veeralingam[1], Sushmee Badhulika[1*]

[1]*Department of Electrical Engineering, Indian Institute of Technology Hyderabad, Hyderabad, 502285, India*

**Corresponding author: E-mail: sbadh@iith.ac.in; Telephone: 040-23018443 Fax 04023016032*

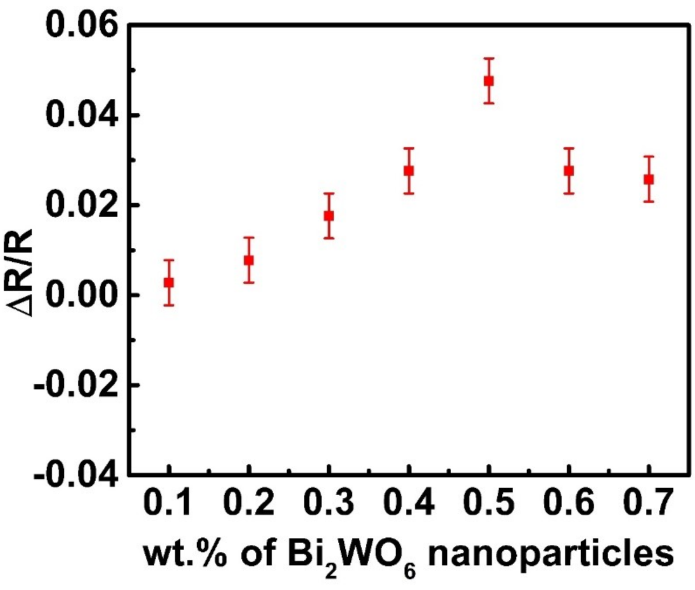

Fig. S1. Response of the Bi_2WO_6 based pH sensor with the solution of pH-6.

Section S1. Structural and chemical analysis of Bi_2WO_6 nanoparticles

The functional group and different vibration modes of Bi_2WO_6 nanoparticles was analyzed using Raman spectroscopy and the spectra was illustrated in **Fig. S2(c)**. Spectra shows the characteristic peaks of Bi_2WO_6 crystal structural with respective vibration modes. The peaks centred at 295 cm^{-1} and 330 cm^{-1} could be attributed to O-W-O stretching vibration and stretching modes of Bi^{3+}. The peak at 410 cm^{-1} associated with the (translational) stretching modes of WO_6^{6-} and 716 cm^{-1} predict the bond length of W-O. The broad peak at 797 cm^{-1} corresponds to the asymmetric A_g stretching of octahedral WO_6^{6-} [1].

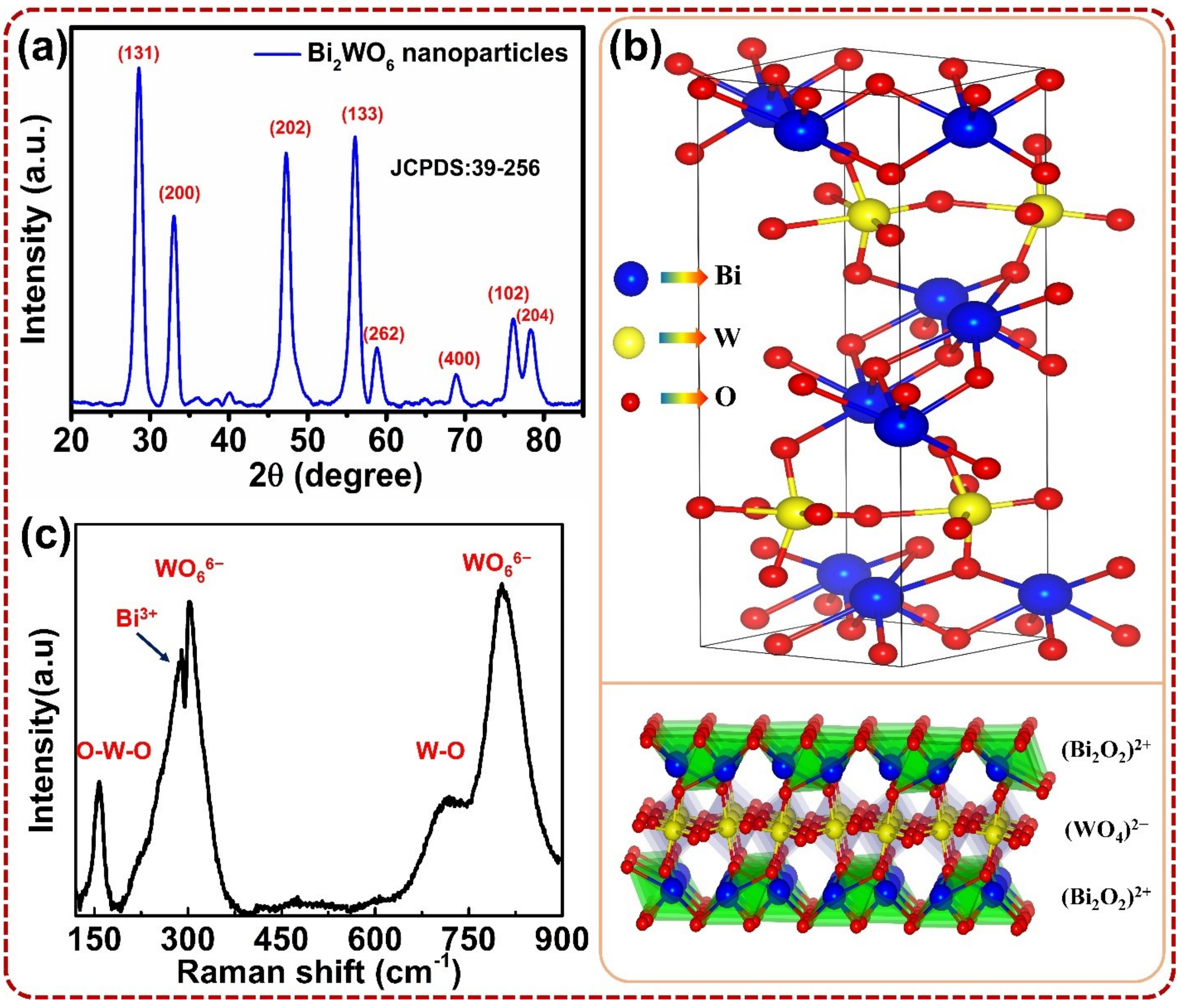

Fig. S2. (a) X-ray diffraction **(b)** layered like structure of orthorhombic Bi_2WO_6. **(c)** Raman spectra of Bi_2WO_6 nanoparticles

Section S2. Morphological analysis of Bi_2WO_6 nanoparticles

The morphological analysis was performed using FE-SEM and micrographs was shown in **Fig. S3(a-d). Fig. S3(a)** illustrates that the Bi_2WO_6 nanoparticles possesses bincocave shape type morphology with controlled size all over the sample. The gaussian distribution of Bi_2WO_6 nanoparticles was performed to determine the average particle size and the particle size of ~86.98 nm was found as shown in the inset of **Fig. S3(a)**. The particle of ~83 nm was observed as illustrated in **Fig. S3(b)**. The elemental analysis and spectra was shown in **Fig. S3(d)** along with the inset table which confirms the presence of only O, W and Bi elements only.

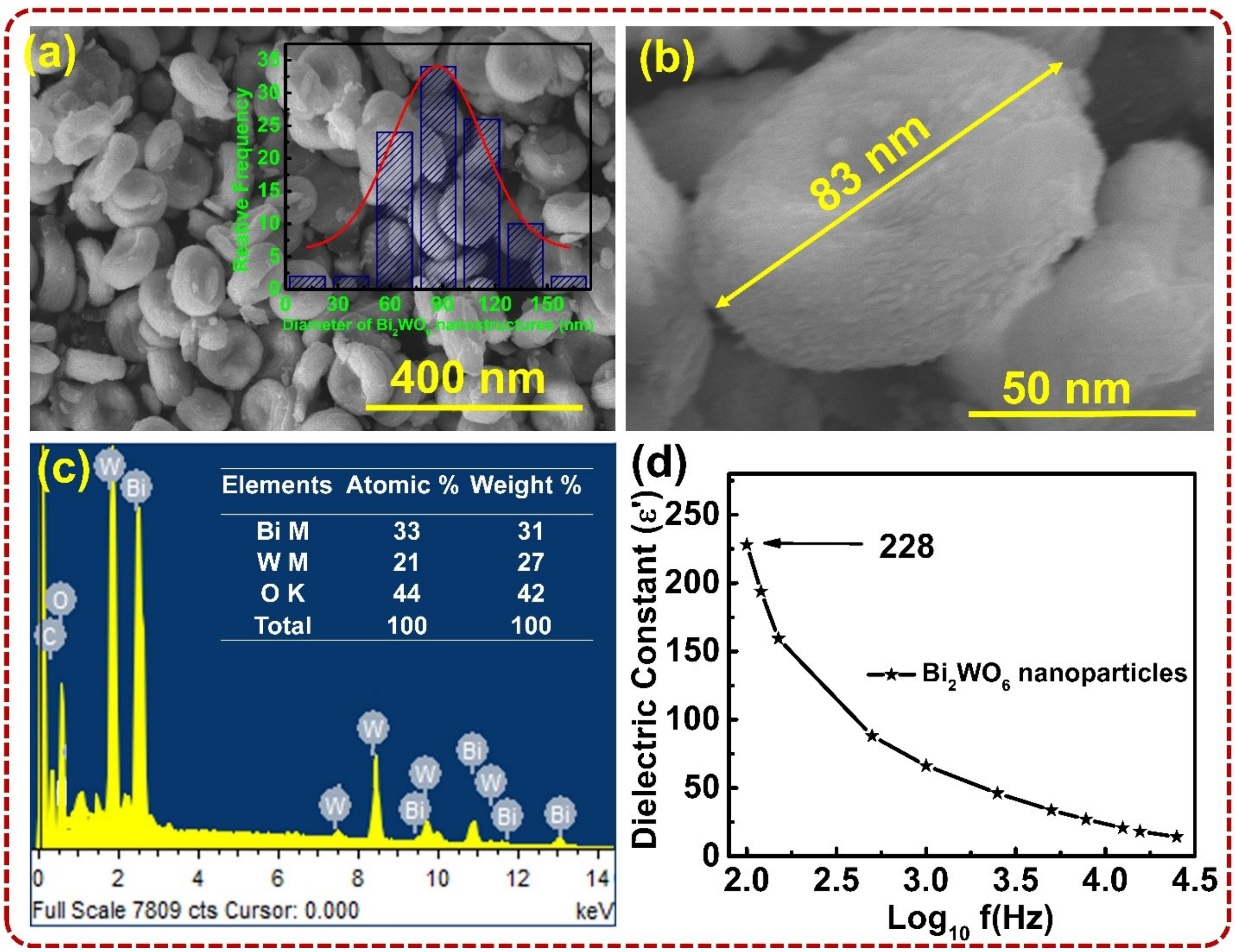

Fig. S3. (a) Low magnification FE-SEM micrographs and (inset) the Gaussian particle distribution of Bi_2WO_6 nanoparticles **(b)** High resolution FE-SEM image of Bi_2WO_6 nanoparticles. **(c)** elemental analysis of Bi_2WO_6 nanoparticles **(d)** Variation of dielectric constant with respect to frequency of Bi_2WO_6 nanoparticles.

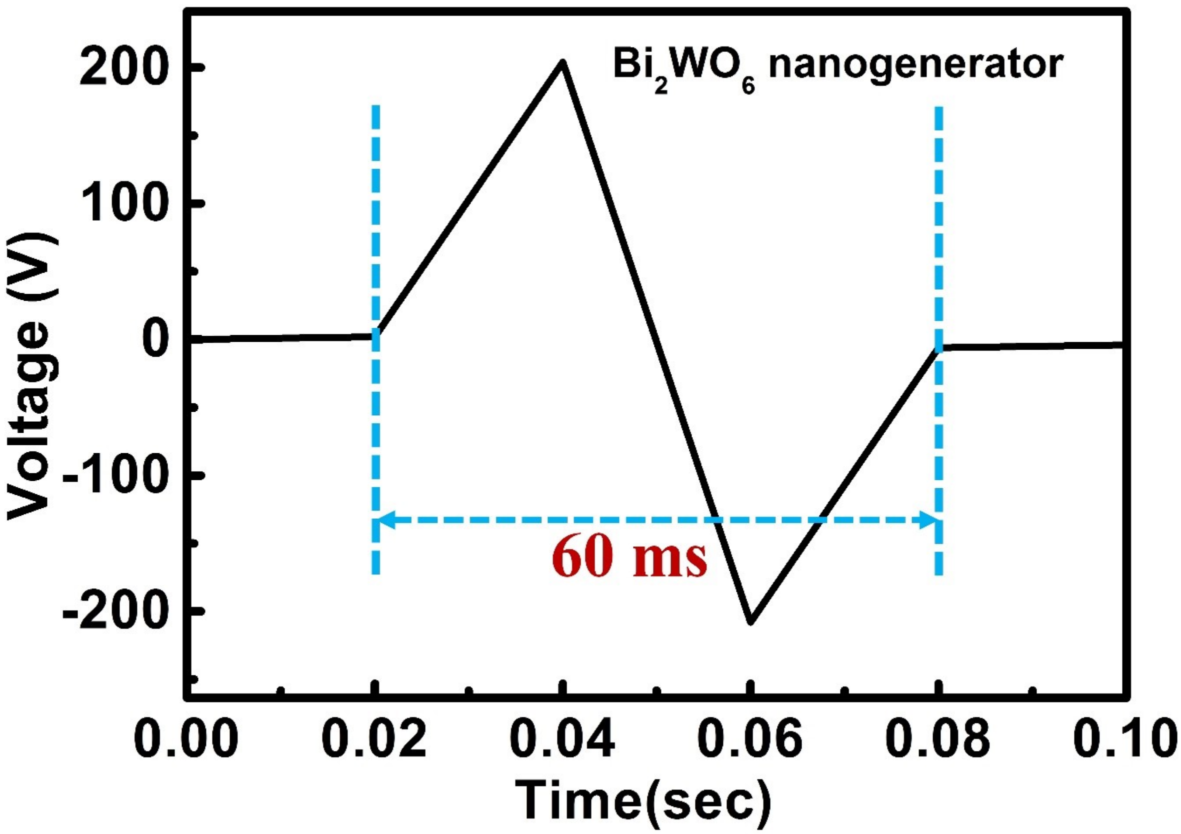

Fig. S4. Response time of Bi_2WO_6: P(VDF-TrFE) triboelectric nanogenerator.

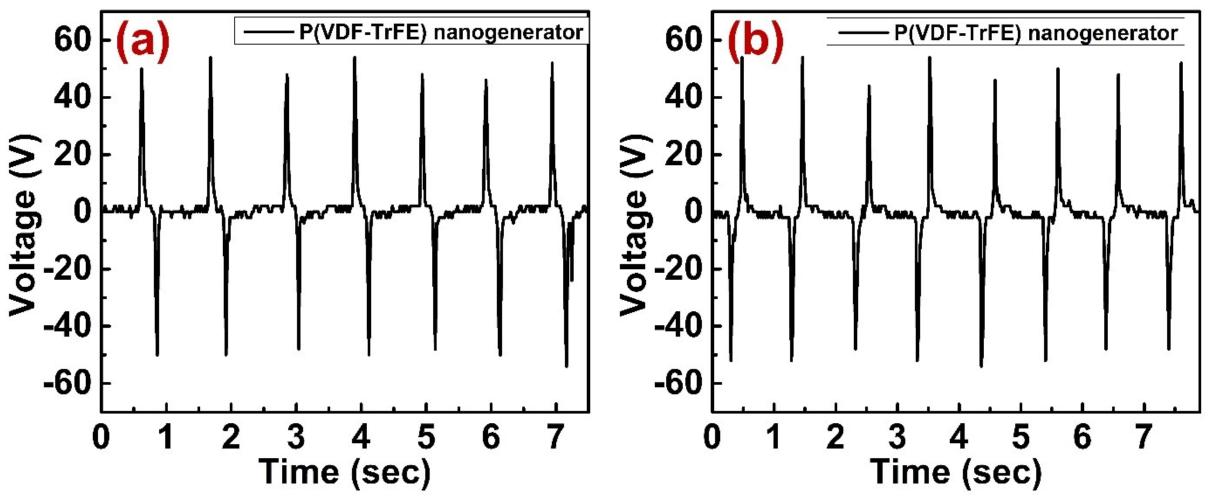

Fig. S5. Output voltage of P(VDF-TrFE) triboelectric nanogenerator under **(a)** forward connection and **(b)** reverse connection condition.

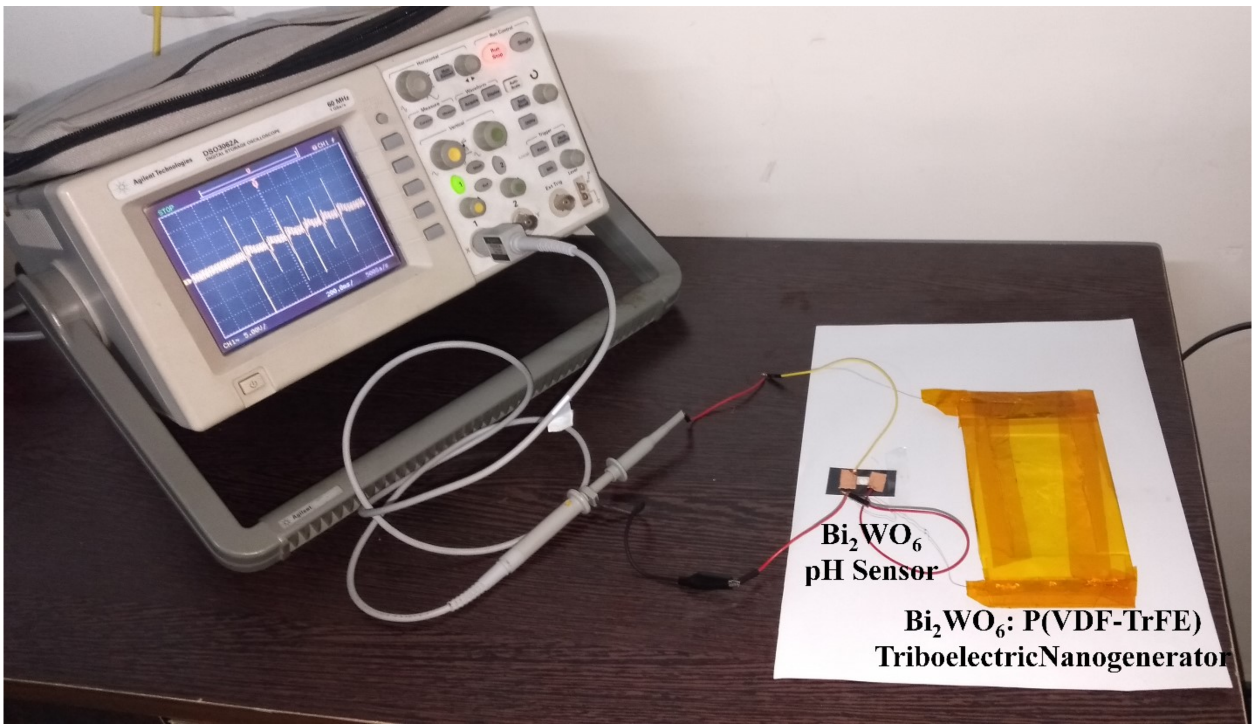

Fig. S6. Pictorial representation of self-power Bi_2WO_6 based pH sensor.

Section S3. Normalized response of Bi_2WO_6 based pH sensor for 30 days

The biocompatibility measurements are typically performed using i) Cell culture assays, ii) toxicity analysis, and iii) in-vitro analysis of isolated cells. However, these experiments are out of scope of this work. Recent reports have demonstrated several applications like biosensors[2, 3], drug-delivery[4], and photocatalysis[5] based on the biocompatibility of Bi_2WO_6. Li et al. demonstrated cell growth related studies to establish the biocompatibility of Bi_2WO_6 nanoparticles [2]. Further, the same study revealed that Bi_2WO_6 nanoparticles are non-toxic and highly biocompatible with human cells. Thus, biocompatibility aspect of Bi_2WO_6 is well validated and documented in previously reported Bi_2WO_6 based literature. The chemical stability of the Bi_2WO_6 based pH sensor was monitored by performing pH sensing studies for 30 days using the same pH sensor, as depicted in the **Fig. S7**. The pH sensor was washed in DI water after every use and stored at 4°C. Ahead of every usage, the sensor was cleaned with buffer solution and exposed to acid and alkali, respectively. The pH sensor displayed a negligible change in response for 30 days, displaying excellent repeatability and no degradation in the pH sensing response upon interaction with acid or alkali.

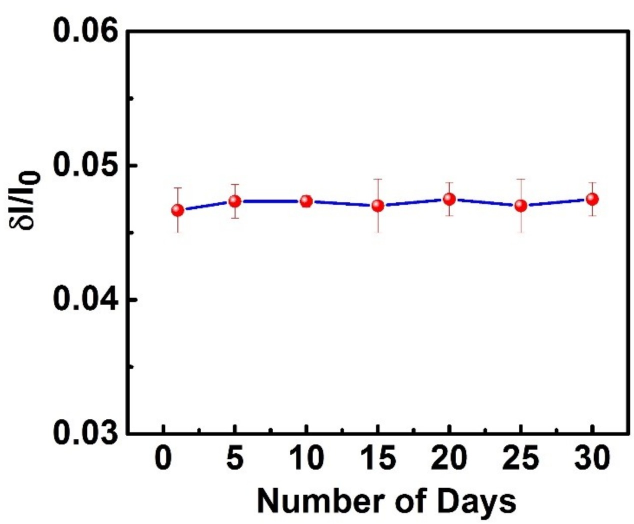

Fig. S7 Normalized response of Bi_2WO_6 based pH sensor for 30 days (N = 5).

Section S4. Raman spectra of Bi_2WO_6 based pH sensor after and before sensing.

Raman studies were performed before and after sensing to evaluate the molecular fingerprint of the pH sensor as shown in **Fig. S8.** Raman spectra shows the characteristic peaks of Bi_2WO_6 crystal structure with respective vibration modes. The peaks centered at 295 cm^{-1} and 330 cm^{-1} can be attributed to O-W-O stretching vibration and stretching modes of Bi^{3+}. The peak at 410 cm^{-1} associated with the (translational) stretching modes of WO_6^{6-} and 716 cm^{-1} predict the bond length of W-O. The broad peak at 797 cm^{-1} corresponds to the asymmetric Ag stretching of octahedral WO_6^{6-}. Moreover, the peaks were replicated exactly for BWO samples obtained after pH sensing. This confirmed absence of acidic or basic functional groups and therefore, negligible degradation of the sensor.

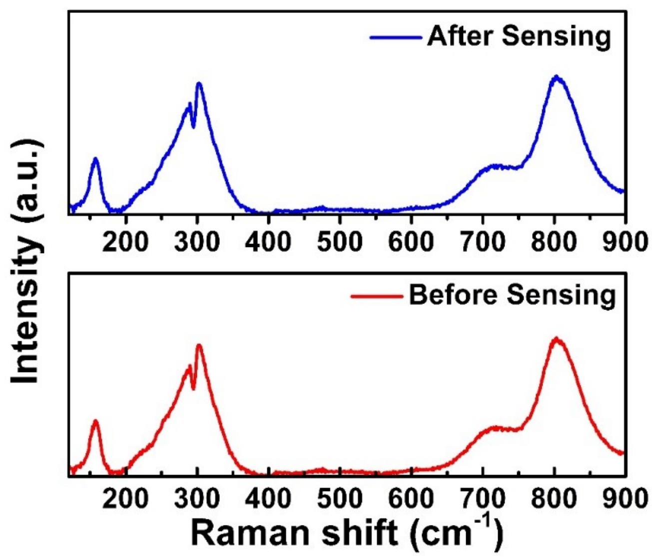

Fig. S8 Raman spectra of Bi_2WO_6 based pH sensor after and before sensing.

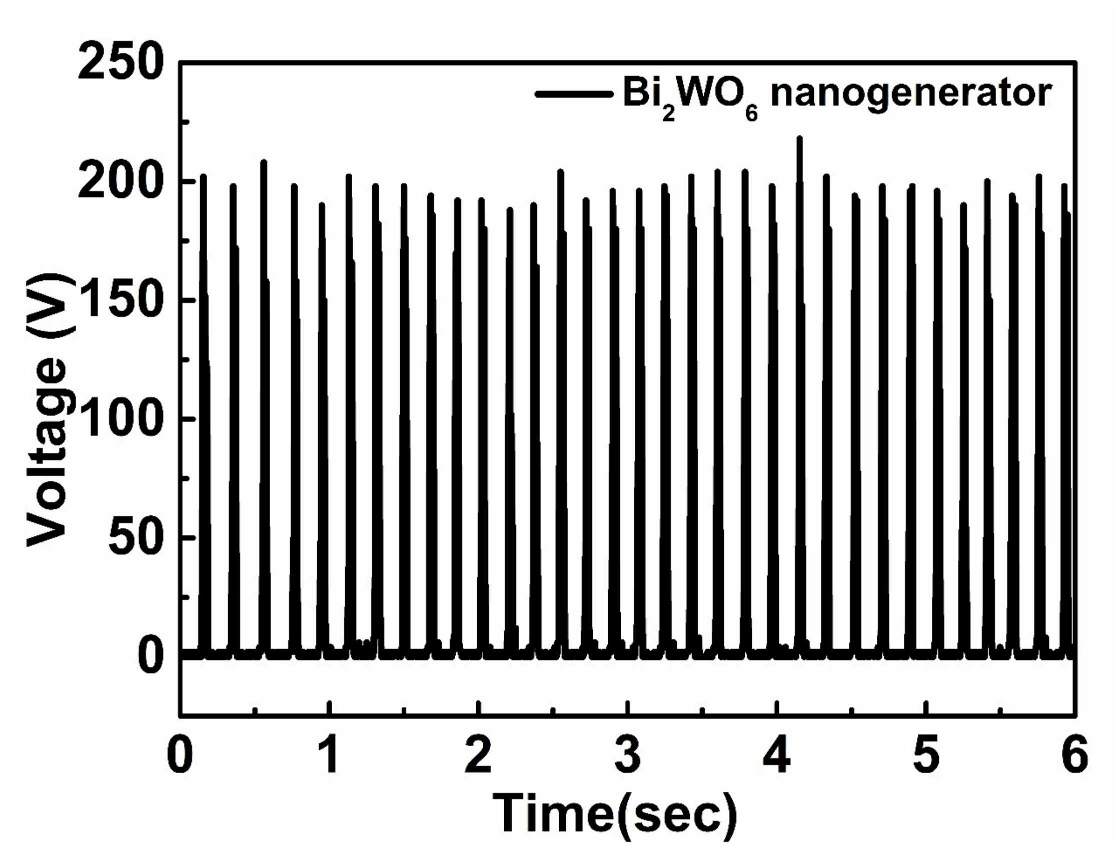

Fig. S9. Rectified output response of Bi_2WO_6: P(VDF-TrFE) triboelectric nanogenerator.

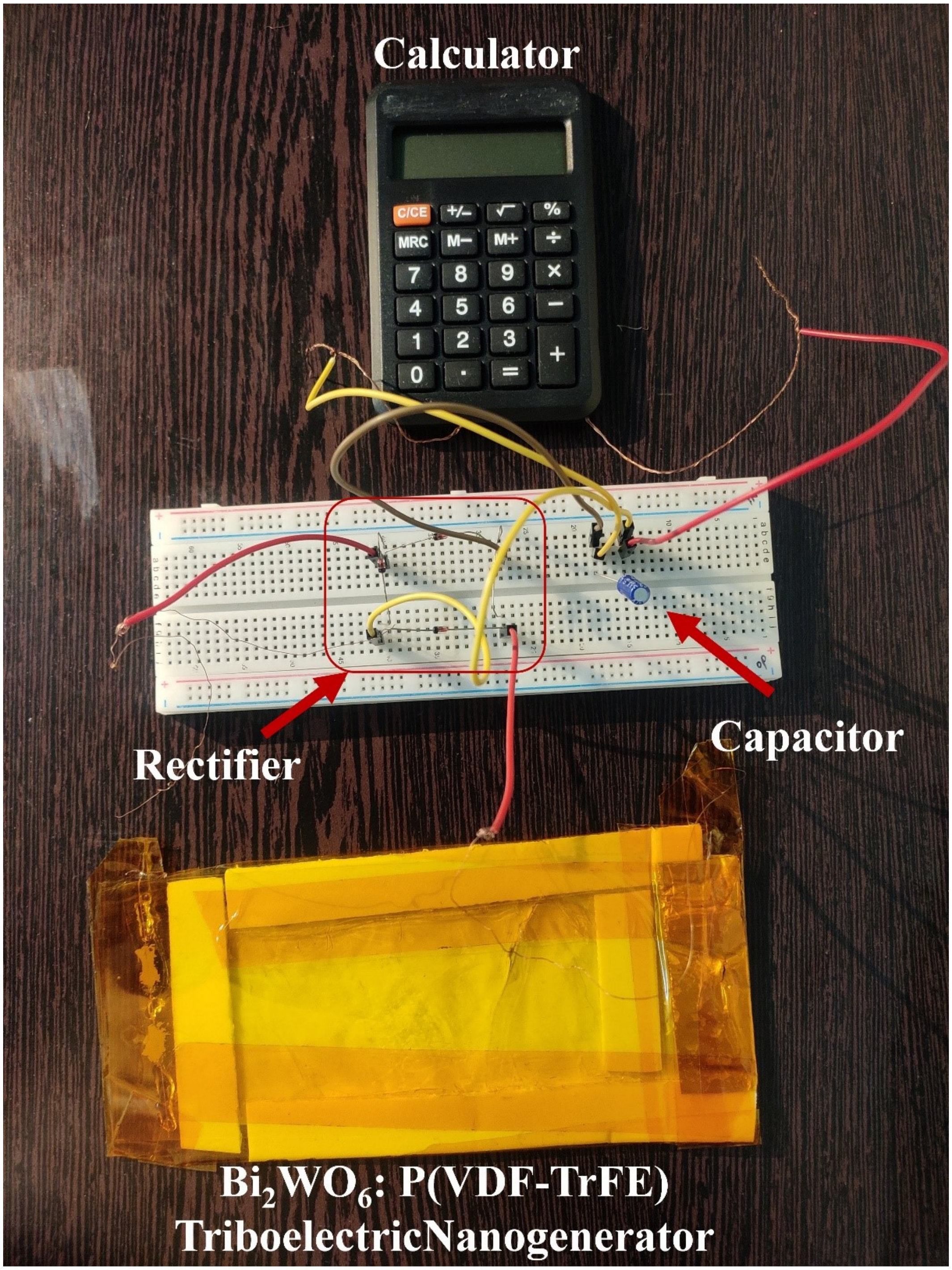

Fig. S10. Pictorial representation of rectification, charging of capacitor and powering of calculator using Bi_2WO_6: P(VDF-TrFE) triboelectric nanogenerator.

Video. V1. Video of powering a calculator using Bi_2WO_6: P(VDF-TrFE) triboelectric nanogenerator.

https://drive.google.com/file/d/1tTO-kpsRecfhC59B8cmq8lxtmJQU8oxI/view?usp=sharing

Section S5. Calculation of cost per self-powered pH sensor:

a) **Calculation for triboelectric Nanogenerator**

1. Price of ITO coated PET substrate (14 x 7) cm^2 = \$ 0.104
2. Cost of chemical utilized per device = \$ 0.816\$
3. Overhead Charges (8%) = \$ 0.08

b) **Calculation of pH sensor**

1. Price of PET substrate (1 x 1) cm^2 = \$ 0.52
2. Cost of chemical utilized per device = \$ 0.404\$
3. Overhead Charges (8%) = \$ 0.04

Total Cost = \$ (1 + 0.964) = \$ 1.964 = ~\$ 2

References

1. A. Etogo, R. Liu, J. Ren, L. Qi, C. Zheng, J. Ning, Y. Zhong and Y. Hu, *Journal of Materials Chemistry A*, 2016, **4**, 13242-13250.
2. B. Li, L. Tan, X. Liu, Z. Li, Z. Cui, Y. Liang, S. Zhu, X. Yang, K. W. Kwok Yeung and S. Wu, *Journal of hazardous materials*, 2019, **380**, 120818.
3. S. Veeralingam and S. Badhulika, *ACS Applied Nano Materials*, 2020, **3**, 12250-12259.
4. A. Kaur, S. Sharma, S. Sood, A. Umar, S. Singh and S. Kansal, *Nanoscience and Nanotechnology Letters*, 2016, **8**, 660-666.
5. Y. Li, H. Wang, J. Xie, J. Hou, X. Song and D. D. Dionysiou, *Chemical Engineering Journal*, 2021, **421**, 129986.